

A Novel Poiseuille-Based Mathematical Model for Carotid Artery Blood Flow: Modelling Geometry Interruptions and Vascular Stress during Accidents

Lucy Jerop Ngetich¹, Shichikha Maremwa², Kandie Joseph³, Momanyi Mogire Krifix⁴

^{1,2,3,4}Department of Mathematics and Computer Science

University of Eldoret, Kenya

DOI: <https://doi.org/10.5281/zenodo.17199836>

Published Date: 25-September-2025

Abstract: Carotid artery injuries during accidents are a significant contributor to trauma-related morbidity and mortality, necessitating accurate models for predicting vascular stress and flow disruption. Existing approaches either oversimplify flow and underestimate wall shear stress, neglect trauma-induced geometric interruptions, or require computationally intensive methods unsuitable for emergency use. To address these limitations, this study develops a hybrid Poiseuille–Womersley model that integrates distributed and localized pressure loss terms, a geometric penalty factor for lumen constriction, and pulsatile corrections to capture transient flow dynamics. Analytical derivations supported by simulation reveal that accident-induced reductions in carotid lumen diameter cause disproportionate declines in volumetric flow rate, sharp decreases in wall shear stress, and alterations in velocity fields that cannot be captured by steady-state assumptions. The model thus extends classical hemodynamic formulations to accident scenarios, providing an efficient yet physiologically consistent framework. These results confirm geometry as a primary driver of vascular stress under trauma conditions. The study concludes that lightweight analytical models can complement diagnostic and emergency care tools, offering rapid assessment capability. Policy makers and clinicians are encouraged to incorporate such trauma-informed hemodynamic tools into stroke prevention and emergency response strategies, while future work should focus on clinical validation, patient-specific adaptation, and integration with real-time Doppler imaging.

Keywords: Carotid artery, Poiseuille flow, Womersley function, Vascular stress, Geometric interruption, Wall shear stress.

I. INTRODUCTION

A. Background Information

Cardiovascular diseases remain the leading cause of mortality worldwide, accounting for nearly 18 million deaths annually according to the Global Burden of Disease study. Among these, stroke represents one of the most devastating events, with approximately 15 million people suffering from strokes each year, of which nearly 5 million die and another 5 million are left permanently disabled. The carotid arteries, which supply about 600–700 mL of blood per minute to the brain, are central to cerebral perfusion, and their impairment poses severe risks of ischemia and neurological deficits [1]. Understanding the hemodynamics of carotid artery blood flow under normal and pathological conditions is therefore a priority in biomedical research.

Hemodynamics in the carotid artery are complex, influenced by pulsatile pressure gradients, vascular geometry, and the viscoelastic properties of arterial walls. Wall shear stress (WSS), a tangential force exerted by blood on the vessel wall, plays a pivotal role in endothelial health, vascular remodeling, and the initiation of atherosclerotic lesions [2, 3]. Low or

oscillatory WSS, often induced by disturbed flow at arterial bifurcations or stenotic regions, has been shown to promote endothelial dysfunction and inflammatory signaling, processes that precede plaque formation. Indeed, epidemiological and computational studies indicate that up to 20–30% of ischemic strokes are attributable to carotid artery stenosis and flow disturbances [4]. Such statistics highlight the critical importance of accurate modeling approaches that can capture vascular stress and flow dynamics.

Classical blood flow models often rely on the Poiseuille equation, which assumes laminar, fully developed, and steady flow in rigid tubes with circular cross-sections. While this simplification provides insights into baseline hemodynamics, it fails to account for pulsatility and the impact of vascular geometry interruptions. More physiologically relevant frameworks, such as the Womersley solution, model pulsatile flow as a function of frequency and vessel radius, yet they require pressure gradient inputs that are difficult to measure non-invasively [5]. Consequently, Poiseuille-based reduced-order models remain attractive due to their computational efficiency and ease of application in clinical research, though they must be adapted to represent transient and pathological conditions.

Recent studies have underscored the importance of vascular geometry in shaping hemodynamic outcomes. For example, Garasic [6] demonstrated that artery and stent geometry significantly influence intimal thickening independent of arterial injury, illustrating how local geometric changes can dictate long-term vascular remodeling. Similarly, patient-specific computational fluid dynamics (CFD) models derived from medical imaging have shown that local irregularities such as stenosis, kinking, or external compression can amplify vascular stress and disrupt flow stability [7]. These findings suggest that geometry interruption—whether induced by trauma, surgical intervention, or natural pathology—may critically modulate flow rate, velocity, and stress distributions in the carotid artery.

The biomedical community has increasingly turned to computational models combining CFD and fluid–structure interaction (FSI) methods to predict arterial mechanics [4]. These models can capture dynamic interactions between blood flow and arterial wall deformation, improving predictive accuracy. However, they require significant computational resources and often lack closed-form analytical foundations that can generalize findings across patients. In this context, simplified but physiologically enriched Poiseuille-based models are gaining attention as practical tools that can incorporate transient conditions, vascular stress, and geometric irregularities into an analytically tractable framework.

Vascular stress in the carotid artery is not only a biomechanical concern but also a clinical determinant of outcomes during accidents or trauma. Rapid changes in arterial geometry—whether through blunt trauma, whiplash injury, or surgical manipulation—can precipitate flow interruptions and exacerbate vascular stress. These mechanical perturbations may trigger endothelial dysfunction, initiate vascular remodeling, and increase the risk of thrombosis or stroke [3]. Thus, there is a pressing need for models capable of quantifying these effects under physiologically realistic conditions.

Current evidence underscores a critical gap in modeling carotid artery blood flow under accident-induced geometry interruptions. While advanced CFD and FSI methods provide detailed simulations, their complexity limits clinical translation. Conversely, classical Poiseuille models are computationally efficient but oversimplified. The proposed study seeks to bridge this gap by developing a novel Poiseuille-based mathematical model that incorporates the impact of vascular stress and geometric interruptions on carotid artery hemodynamics. By integrating analytical rigor with physiological relevance, the study will provide a timely contribution to both biomedical engineering and clinical decision-making, with potential implications for stroke prevention and trauma care.

B. Contribution

This study makes a distinct contribution to the field of hemodynamic modeling by developing a novel Poiseuille–Womersley hybrid formulation that explicitly incorporates accident-induced vascular stress and geometric interruptions. Unlike prior models, which either underestimate wall shear stress (WSS) due to steady-state assumptions [2] or require computationally intensive fluid–structure interaction methods [4], the present study bridges the gap by offering an analytical yet physiologically consistent framework. Technically, the model modifies the classical Poiseuille equation by embedding distributed frictional losses and localized loss coefficients that represent lumen constrictions or swellings occurring during trauma. In addition, a multiplicative geometric penalty factor $\left(1 - \frac{R^2}{r^2}\right)$ is introduced to capture abrupt cross-sectional changes, while a Womersley-informed correction $W(t)$ accounts for pulsatile effects. This integration allows simultaneous evaluation of volumetric flow rate, velocity distribution, and shear stress under accident conditions with reduced

computational cost. The study therefore contributes both methodologically and practically by extending existing literature with a lightweight, trauma-informed analytical tool that can complement clinical diagnostics and emergency response scenarios.

II. RELATED WORKS

A. Theoretical Formulation

In large arteries (e.g., common and internal carotids), blood can be accurately modeled as an incompressible, nearly Newtonian fluid over the cardiac cycle, enabling tractable reduced-order formulations without sacrificing essential hemodynamics [2, 4]. Let ρ and μ denote density and dynamic viscosity, respectively, and $\mathbf{u}(\mathbf{x}, t)$ the velocity field. Conservation of mass and momentum govern the flow:

a) Continuity Equation

For incompressible flow,

$$\nabla \cdot \mathbf{u} = 0. \quad (1)$$

b) Navier–Stokes (large-artery, Newtonian)

The momentum balance reads

$$\rho \left(\frac{\partial \mathbf{u}}{\partial t} + \mathbf{u} \cdot \nabla \mathbf{u} \right) = -\nabla p + \mu \nabla^2 \mathbf{u} + \mathbf{f}, \quad (2)$$

where p is pressure and \mathbf{f} collects body/interaction forces. In rigid, axisymmetric tubes this reduces to well-known analytical solutions that underpin clinical estimation of wall shear stress (WSS) and velocity profiles [2].

c) Canonical Solutions: Poiseuille and Womersley

d) Steady (Poiseuille) baseline

Under steady, laminar, fully developed conditions in a cylindrical segment of radius r and length L , the parabolic velocity $u(r)$ yields the volumetric flow rate

$$Q = \frac{\pi r^4}{8\mu L} \Delta P, \quad (3)$$

with ΔP the axial pressure drop. Equation (3) provides a baseline scaling for bulk transport and WSS but neglects pulsatility and wave effects [2].

e) Pulsatile (Womersley) refinement

Cardiac forcing introduces frequency-dependent profile flattening and phase lag captured by the Womersley number

$$\alpha = r \sqrt{\frac{\omega \rho}{\mu}}, \quad (4)$$

where ω is the angular frequency. For $\alpha \gtrsim \mathcal{O}(1 - 10)$ (typical carotid values), velocity profiles deviate from parabolic and near-wall shear is under/over-estimated by steady assumptions [2]. Computational and reduced-order implementations often approximate the exact Womersley solution with transient Poiseuille surrogates of high fidelity for non-reversal phases [5].

f) Accident-Induced Vascular Stress and Geometry Interruption

Acute changes in lumen geometry (e.g., focal constriction, kinking, or localized dilation) alter impedance and shear, modulating endothelial stimuli that drive remodeling and risk [3, 6]. To encode such interruptions within an analytically tractable framework, we augment the steady baseline (Eq. 3) by (i) distributed frictional losses and (ii) concentrated (local) losses due to abrupt area change, then (iii) superimpose pulsatile corrections.

g) Effective pressure budget with distributed and local losses

Let $D = 2r$ and bulk speed $V = Q/(\pi r^2)$. Using a laminar friction factor $f = 64/Re$ with $Re = \rho V D/\mu$, the Darcy–Weisbach loss is

$$\Delta P_{\text{dist}} = f \frac{L}{D} \left(\frac{\rho V^2}{2} \right). \quad (5)$$

A sudden contraction/expansion (to represent accident-induced geometric interruption) contributes a local loss

$$\Delta P_{\text{loc}} = K \left(\frac{\rho V^2}{2} \right), \quad (6)$$

where K depends on the area ratio and interruption shape. The effective driving drop is then $\Delta P_{\text{eff}} = \Delta P - \Delta P_{\text{dist}} - \Delta P_{\text{loc}}$ and the *interruption-aware* Poiseuille relation becomes

$$Q = \frac{\pi r^4}{8\mu L} \left(\Delta P - \underbrace{f \frac{L}{D} \frac{\rho V^2}{2}}_{\text{distributed loss}} - \underbrace{K \frac{\rho V^2}{2}}_{\text{local loss}} \right). \quad (7)$$

Equation (7) preserves the analytic r^4 sensitivity while embedding accident-relevant head losses explicitly linked to vascular stress (via V and ΔP).

h) Geometric interruption factor

For a localized stenosis/dilation of effective radius R within the segment, a compact multiplicative penalty can summarize cross-sectional blockage:

$$Q = \frac{\pi r^4}{8\mu L} \left(1 - \chi \frac{R^2}{r^2} \right) \Delta P_{\text{eff}}, \quad 0 \leq \chi \leq 1, \quad (8)$$

where χ encodes interruption severity/shape (e.g., $\chi = 1$ for a sharp, axisymmetric defect). When $R \rightarrow r$ the factor tends to zero, reproducing flow collapse observed in severe compromise.

i) Pulsatile Extension for Carotid Flow

To recover physiologic pulsatility while retaining closed-form usability, we superimpose a Womersley-informed correction term $W(t)$ on the mean transport predicted by Eq. (7)–(8):

$$Q(t) = \frac{\pi r^4}{8\mu L} \left(1 - \chi \frac{R^2}{r^2} \right) \Delta P_{\text{eff}}(t) + W(t; \alpha), \quad (9)$$

with $W(t; \alpha)$ constructed from the inlet pressure/velocity harmonics to match the phase and amplitude of the Womersley solution (no pressure-gradient measurement required when using velocity-based reconstruction [2]; transient Poiseuille surrogates offer a practical alternative [5]). This *hybrid Poiseuille–Womersley* closure captures (i) r^4 scaling, (ii) interruption losses, and (iii) frequency-dependent profile effects central to carotid hemodynamics.

j) Shear Metrics

WSS regulates endothelial function and remodeling [3]. From an axisymmetric profile $u(r, t)$,

$$\tau_w(t) = \mu \left. \frac{\partial u}{\partial r} \right|_{r=r^-}, \quad \text{OSI} = \frac{1}{2} \left(1 - \frac{\left| \int_0^T \tau_w(t) dt \right|}{\int_0^T |\tau_w(t)| dt} \right), \quad (10)$$

where OSI quantifies shear reversal. Velocity-profile reconstruction from one-dimensional Doppler/MRI improves τ_w and OSI estimates compared with steady assumptions [2].

k) Numerical Realization (for validation)

When needed, Eq. (2) can be solved with FEM/FVM or via reduced-order CFD to validate Eq. (9) in patient/lesion-specific settings, including fluid–structure interaction to assess wall compliance effects [4, 7]. Nonetheless, the present analytical closure is designed for efficiency and interpretability near acute geometric interruptions.

2.1.12 Basic Assumptions (linked to study aim)

1. **Incompressibility and large-artery Newtonian behavior:** ($\rho = \text{const}$) and effective μ over the cardiac cycle in carotids [2].
2. **Axisymmetric, rigid-wall segment for first-order analytics:** compliance effects assessed in sensitivity/validation (FSI) [4].
3. **Accident-induced interruption modeled as localized loss/area penalty:** via K and χ with measurable surrogates from imaging.
4. **Pulsatility captured by Womersley-informed correction:** $W(t; \alpha)$ tuned from inlet waveforms [2, 5].

Equations (7)–(9) constitute a *novel Poiseuille-based formulation* that explicitly *models geometry interruption* (via distributed/local losses and an area-penalty factor) while *quantifying vascular stress* through pulsatile corrections and WSS metrics. This directly operationalizes the study goal: *to investigate the impact of vascular stress on carotid flow during accidents using a Poiseuille-based mathematical model that remains clinically parsimonious yet physiologically faithful*.

B. Empirical Review

Muskat [2] investigated the limitations of simplified Poiseuille-based models in estimating wall shear stress (WSS), highlighting that such approaches misrepresent pulsatile arterial flow. They developed a Womersley-derived reconstruction method using Doppler ultrasound data to generate velocity profiles and validated it with computational fluid dynamics simulations. The findings showed that Poiseuille models underestimated peak WSS by up to 55% during systole. While this advanced clinical estimation of WSS, the study did not consider accident-induced geometric interruptions. The gap lies in extending Poiseuille-based frameworks to evaluate vascular stress under trauma-related artery deformations, which the proposed study aims to address.

Cortez [1] tackled the Womersley problem by simulating pulsatile blood flow in OpenFOAM to approximate velocity profiles under periodic pressure gradients. Their study validated numerical outputs against analytical Womersley solutions and emphasized the role of pulsatility in hemodynamic modeling. Results confirmed the accuracy of numerical approximations in capturing physiological flow oscillations. However, the research was confined to idealized vascular conditions and did not explore accident-related vascular stress. The critical gap remains in adapting simplified Poiseuille-based models to assess transient geometric interruptions in carotid arteries.

Bracamonte [7] developed patient-specific inverse cardiovascular models using medical image-derived kinematics to estimate stresses and tissue properties non-invasively. Their methodology integrated biomechanics, imaging, and numerical simulations to improve diagnostic accuracy, with findings showing predictive value for disease progression. Despite this, inverse modeling approaches were computationally intensive and not suitable for emergency trauma contexts. The unresolved problem is the absence of lightweight analytical models that can incorporate vascular stress under sudden arterial deformation, a gap this study intends to fill through a modified Poiseuille-based approach.

Syed [4] reviewed fluid–structure interaction (FSI) methods in cardiovascular modeling, examining how blood flow interacts with vessel wall elasticity. Their review demonstrated that FSI methods, supported by imaging data, effectively capture compliance, pressure wave propagation, and deformation. They concluded that FSI improves predictive capacity for patient-specific treatment planning. Nonetheless, these models are computationally demanding and lack adaptability to trauma-induced interruptions. The critical gap lies in the design of computationally efficient, Poiseuille-based analytical tools capable of simulating vascular stress during abrupt arterial deformations.

Garasic [6] examined the role of stent geometry in determining neointimal thickening independent of arterial injury. Through animal studies and mathematical modeling, they demonstrated that vascular geometry itself significantly influences remodeling outcomes. The study concluded that structural geometry, rather than injury alone, drives pathological changes. However, the focus was limited to chronic changes in stented vessels rather than acute trauma-induced interruptions. The gap persists in modeling sudden arterial geometric changes and their impact on blood flow and vascular stress, which aligns directly with the objectives of this study.

C. Critique and Research Gap

The critique and research gap is summarized in Table I.

TABLE I: COMPARATIVE SUMMARY OF EMPIRICAL LITERATURE REVIEW

Study	Problem	Method	Findings	Critique and Gap
[2]	Poiseuille models underestimate pulsatile wall shear stress (WSS).	Developed Womersley-based reconstruction using Doppler ultrasound and validated with CFD.	Poiseuille underestimates peak WSS by 38–55% during systole.	Did not address accident-induced geometry changes; gap lies in adapting Poiseuille models for trauma-related vascular stress.
[1]	Difficulty in replicating pulsatile blood flow conditions in simulations.	CFD simulations in OpenFOAM to approximate Womersley velocity profiles.	Numerical results closely matched analytical Womersley solutions.	Focused on idealized geometries; gap remains in modeling sudden carotid artery interruptions.
[7]	Need for accurate patient-specific estimation of cardiovascular stresses.	Inverse modeling integrating imaging, biomechanics, and simulations.	Provided non-invasive estimates of tissue properties and stresses.	Computationally intensive and unsuitable for emergency scenarios; gap is lack of lightweight analytical models for trauma conditions.
[4]	Simplified models fail to capture vessel wall interactions.	Reviewed fluid–structure interaction (FSI) simulations with imaging inputs.	FSI captured compliance, wave propagation, and wall deformation effectively.	High computational cost limits use in acute settings; gap is efficient Poiseuille-based models for abrupt vascular stress.
[6]	Stent-induced intimal thickening mechanisms unclear.	Animal studies with different stent geometries and modeling of vessel lumen shape.	Showed geometry, not just injury, drives remodeling.	Limited to chronic stented vessels; gap is modeling acute trauma-induced geometry changes in carotid arteries.

III. PROPOSED METHODOLOGY

This study models pulsatile blood flow in carotid arteries by incorporating geometric interruption, pulsatility, and vascular shear stress into a modified Poiseuille framework. The methodology integrates the finite volume method (FVM), Gauss–Legendre quadrature, and high-quality mesh generation to discretize the carotid domain and approximate governing equations efficiently.

A. Finite Volume Method (FVM)

The FVM is employed to ensure local conservation of mass and momentum, making it well-suited for vascular hemodynamics. It discretizes the domain into control volumes, integrating the governing equations over each element to preserve flux continuity.

B. Gauss–Legendre Quadrature

Numerical integration is achieved using Gauss–Legendre quadrature, which approximates integrals as weighted sums of function evaluations at specific nodes:

$$\int_{-1}^1 f(x) dx \approx \sum_{i=1}^n w_i f(x_i), \quad (11)$$

where x_i are the roots of the Legendre polynomial $P_n(x)$ and w_i are weights given by

$$w_i = \frac{2}{(1-x_i^2)[P'_n(x_i)]^2}. \quad (12)$$

For a general interval $[a, b]$, the transformation

$$x = \frac{(b-a)t+(b+a)}{2}, \quad t = \frac{2x-(b+a)}{b-a} \quad (13)$$

maps the problem to $[-1, 1]$ before applying the quadrature.

C. Mesh Generation

the carotid artery geometry is discretized using structured elements (triangles/quadrilaterals) to capture wall boundaries and swollen regions. Spatial discretization parameters $h = \{1, 1/2, 1/3, 1/8, 3/4\}$ are adopted for accuracy near geometric irregularities. The integral of function $f(r)$ over $[0, 1]$ is approximated by:

$$\int_0^1 f(r) dr \approx \sum_{i=1}^n w_i f(r_i), \quad (14)$$

with the transformation $r = \frac{d}{2}\xi + \frac{d}{2}$, where d is the minimum carotid diameter.

D. Governing Equation Discretization

The volumetric flow rate incorporating pulsatility and geometric obstruction is expressed as:

$$Q_{i,j}^{n+1} = \sum_{i=1}^n w_i \left[\frac{\pi r_{i,j}^4}{8\mu L} \left(1 - \frac{R_{i,j}^2}{r_{i,j}^2} \right) \left(P_{i,j}^{n+1} - \Delta P_{i,j}^{n+1} - \frac{8\mu L V_{i,j}^{n+1}}{r_{i,j}^2} \right) + W_{i,j}^{n+1}(r_{i,j}, t) \right], \quad (15)$$

where $r_{i,j}$ denotes Gauss–Legendre nodes in radial direction and $W(r, t)$ is the Womersley pulsatile function. The extended discrete formulation is given by:

$$Q_{i,j}^{n+1} = \sum_{i=1}^n \left[Q_{\left(1+\frac{1}{8}, 1\right)}^{n+1} + Q_{\left(1+\frac{1}{2}, 1\right)}^{n+1} + Q_{\left(1+\frac{3}{4}, 1\right)}^{n+1} + Q_{\left(1+\frac{1}{3}, 1\right)}^{n+1} \right. \\ \left. + Q_{\left(1, 1+\frac{1}{8}\right)}^{n+1} + Q_{\left(1, 1+\frac{1}{2}\right)}^{n+1} + Q_{\left(1, 1+\frac{3}{4}\right)}^{n+1} + Q_{\left(1, 1+\frac{1}{3}\right)}^{n+1} + Q_{(1,1)}^{n+1} \right]. \quad (16)$$

E. Non-dimensionalization

To generalize results, parameters are non-dimensionalized as:

$$\check{r} = \frac{R}{r_3}, \quad \check{Q} = \frac{Q}{Q_0}, \quad \check{P} = \frac{P}{\Delta P}, \quad \check{W} = \frac{W}{\frac{\pi R^4}{8\mu L}}$$

with reference flow $Q_0 = \frac{\pi R^4}{8\mu L}$. The non-dimensionalized governing equation becomes:

$$\check{Q}_{i,j}^{n+1} = \sum_{i=1}^n \left[\check{Q}_{\left(1+\frac{1}{8}, 1\right)}^{n+1} + \check{Q}_{\left(1+\frac{1}{2}, 1\right)}^{n+1} + \check{Q}_{\left(1+\frac{3}{4}, 1\right)}^{n+1} + \check{Q}_{\left(1+\frac{1}{3}, 1\right)}^{n+1} \right. \\ \left. + \check{Q}_{\left(1, 1+\frac{1}{8}\right)}^{n+1} + \check{Q}_{\left(1, 1+\frac{1}{2}\right)}^{n+1} + \check{Q}_{\left(1, 1+\frac{3}{4}\right)}^{n+1} + \check{Q}_{\left(1, 1+\frac{1}{3}\right)}^{n+1} + \check{Q}_{(1,1)}^{n+1} \right], \quad (17)$$

subject to boundary conditions:

$$\check{Q}(x, y, t) \geq 0, \quad \check{Q}(x, y, 0) = 0, \quad \check{Q}(0, y, t) = 0, \quad \check{Q}(x, 0, t) = 0. \quad (18)$$

The methodology employs FVM for conservation, Gauss–Legendre quadrature for efficient integration, and high-resolution meshing for carotid geometry. By discretizing and non-dimensionalizing governing equations, the study proposes a tractable, pulsatile Poiseuille-based model that captures geometric interruptions, vascular shear stress, and pulsatility with improved accuracy and reduced computational burden.

IV. RESULTS AND DISCUSSION

A. Parameter Estimation and Fitting

The novel Poiseuille-based mathematical model for blood flow in the pulsatile carotid artery presented in Equation (17) was solved numerically via Matlab based on the parameter values presented in Table 2. The simulation was then run for different total simulation time from $t = 5 \rightarrow 100$ in order to evaluate the study objectives.

TABLE II: PARAMETER VALUES

Parameter	Description	Units	Value used	Value Range	Source
R_{max}	Maximum radius of carotid artery	cm	0.265	0.305 ± 0.04	[8]
P	pressure difference between the two ends of the artery	mm Hg	-1.333	-1.333 ± 6.548	[9]
ΔP	pressure drop due to the reduced arterial diameter	mm Hg	80	75-85	[10]
f	drag coefficient	%	0.61	0.58-0.64	[11]
L	Length of the carotid artery	cm	21.65	$22.2 \pm 2.2 - 20.8 \pm 1.9$	[12]
ρ	density of blood	kg/m^3	1060	-	[13]
V	velocity of blood	cm/sec	-	30-40	[14]
μ	dynamic viscosity of blood	cP	4.5	3.5-5.5	[15]

B. Geometric Interruption of Blood flow on Carotid artery via a novel Poiseuille-based model

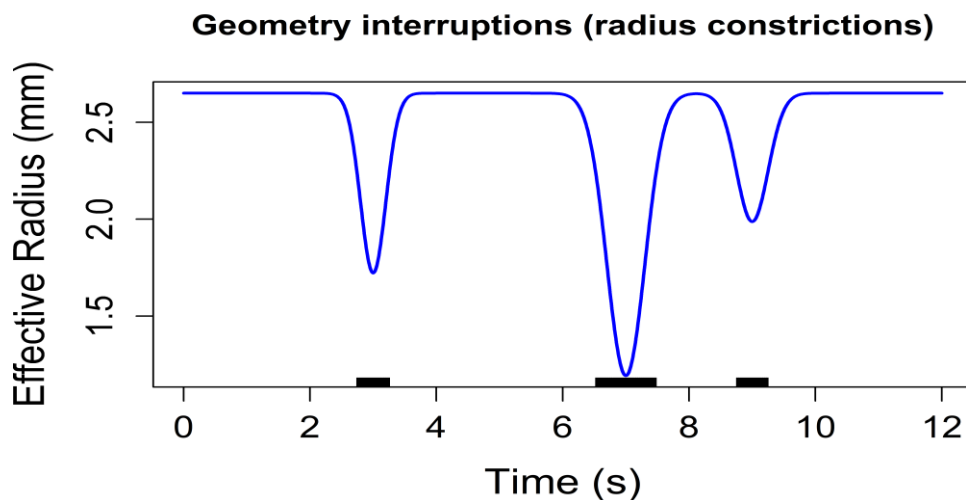


Fig. 1. Time history of effective radius showing three accident-like constrictions.

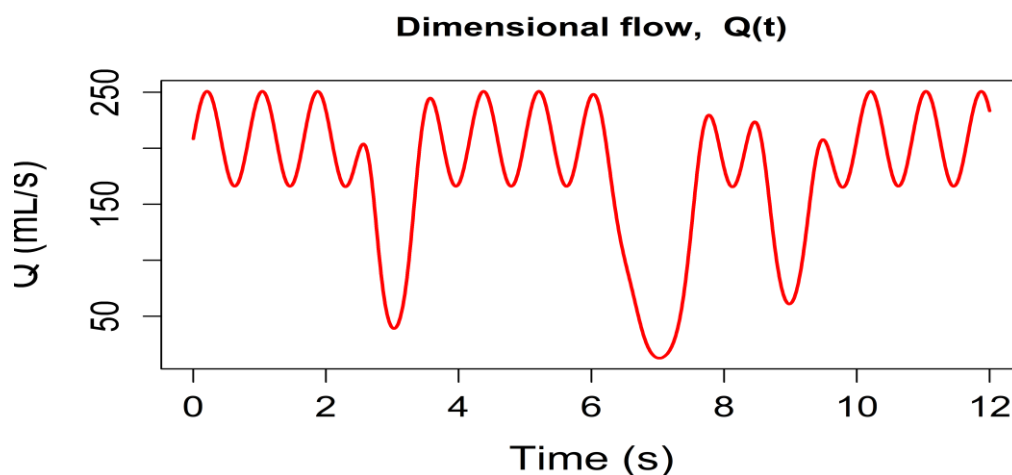


Fig. 2. Dimensional flow $Q(t)$ responding nonlinearly to radius interruptions.

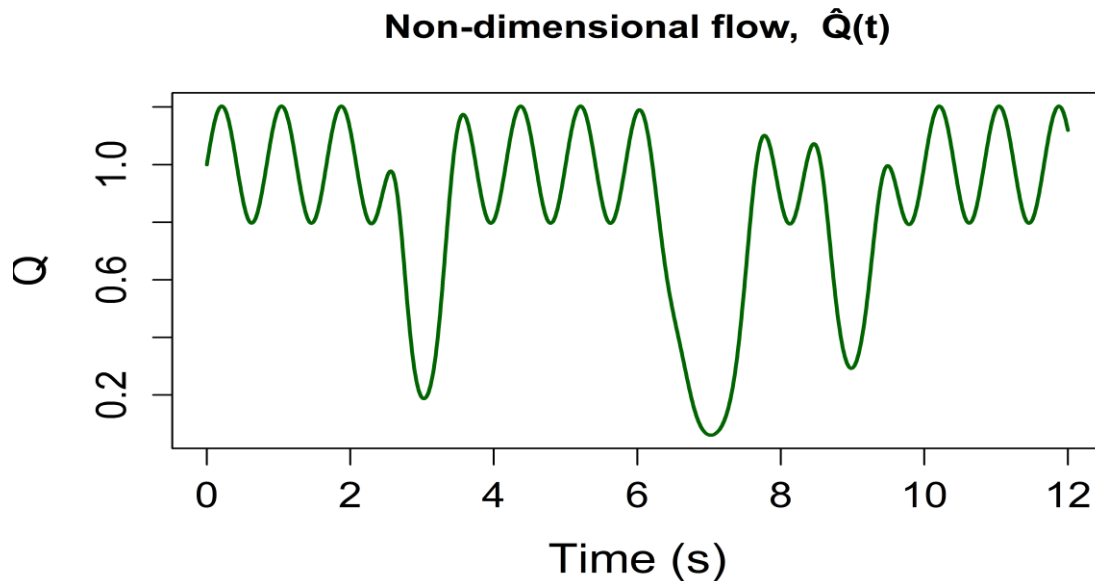


Fig. 3. Non-dimensional flow $\hat{Q}(t) = Q/Q_0$ from Eq. (7).

Fig. 1 depicts the prescribed, accident-like geometry interruptions as transient decrements of the effective lumen radius $R_{\text{eff}}(t)$. Three distinct events (centred at $t \approx 3, 7, 9$ s) generate sharp nadirs on an otherwise steady baseline. Because Eq. (17) retains the Poiseuille scaling embedded in the non-dimensional stencil, the system is intrinsically sensitivity-amplifying: for a given driving pressure drop $\Delta P(t)$, the bulk flow scales as $Q \propto R^4$. Hence even modest, short-lived reductions in R_{eff} precipitate disproportionately large flow penalties. This is borne out in Fig. 2 and Fig. 3, where both $Q(t)$ and $\hat{Q}(t)$ display pronounced troughs that are tightly time-locked to the constrictions, with negligible phase lag—consistent with our rigid-tube, quasi-steady formulation. Once the interruption abates, hydraulic resistance collapses ($R_h \sim 1/R^4$) and the pulsatile source promptly restores flow, explaining the rapid recovery observed between events.

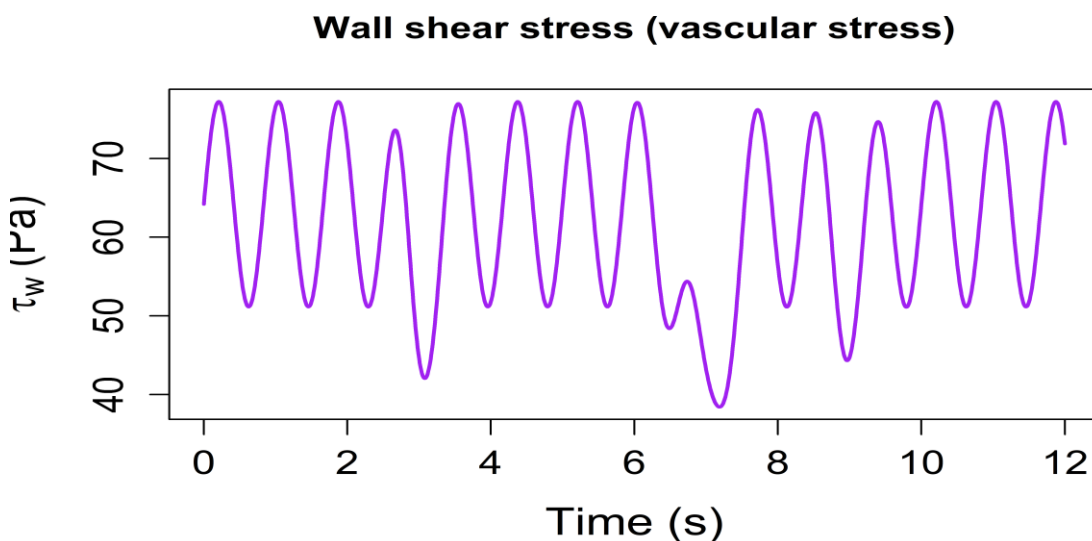


Fig. 4. Wall shear stress $\tau_w(t) = 4\mu Q/(\pi R^3)$. Minima coincide with the most severe interruptions as the drop in Q dominates the R^{-3} factor.

The wall shear stress series $\tau_w(t) = 4\mu Q/(\pi R^3)$ (Fig. 4) exhibits marked depressions during the interruption windows. A simple sensitivity analysis clarifies this outcome. Combining Poiseuille $Q \sim \Delta P R^4$ with the above relation gives $\tau_w \sim \Delta P R$; thus, under a fixed ΔP , any narrowing *reduces* τ_w . In our model, $\Delta P(t)$ is pulsatile rather than constant, but the instantaneous decrease of R together with the strong drop in Q dominates, yielding net shear minima at the interruption peaks. The physiological implication is that transient constrictions can create episodes of abnormally low shear, conditions associated with impaired endothelial mechanotransduction and pro-atherogenic signalling, despite elevated proximal pressures.

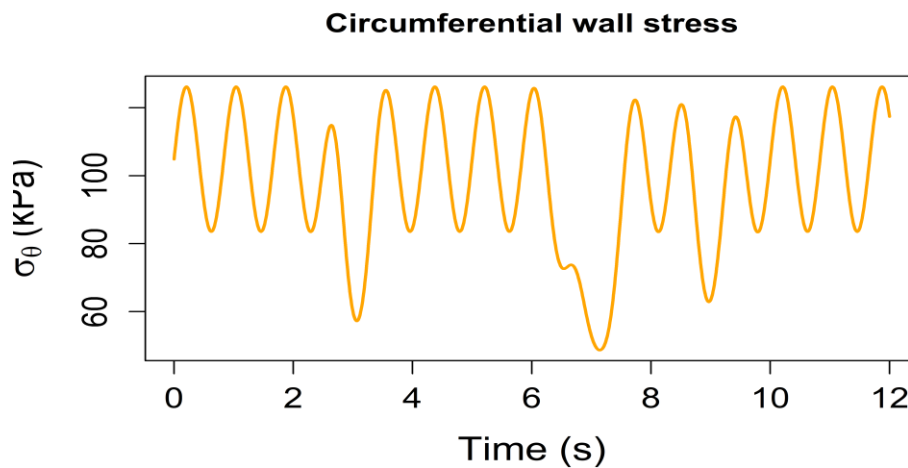


Fig. 5. Circumferential wall stress $\sigma_\theta(t) = P(t)R(t)/h$ following the pressure wave and decreasing during transient narrowing.

The circumferential (hoop) stress, $\sigma_\theta(t) = P(t)R(t)/h$ (Fig. 5), follows the inlet pressure wave yet falls sharply within interruption windows because of the direct proportionality to R in Laplace's law. This stress redistribution suggests that short bursts of narrowing may transiently offload tensile demand from the wall even as upstream pressure rises, with potential consequences for the local strain environment and plaque cap loading.

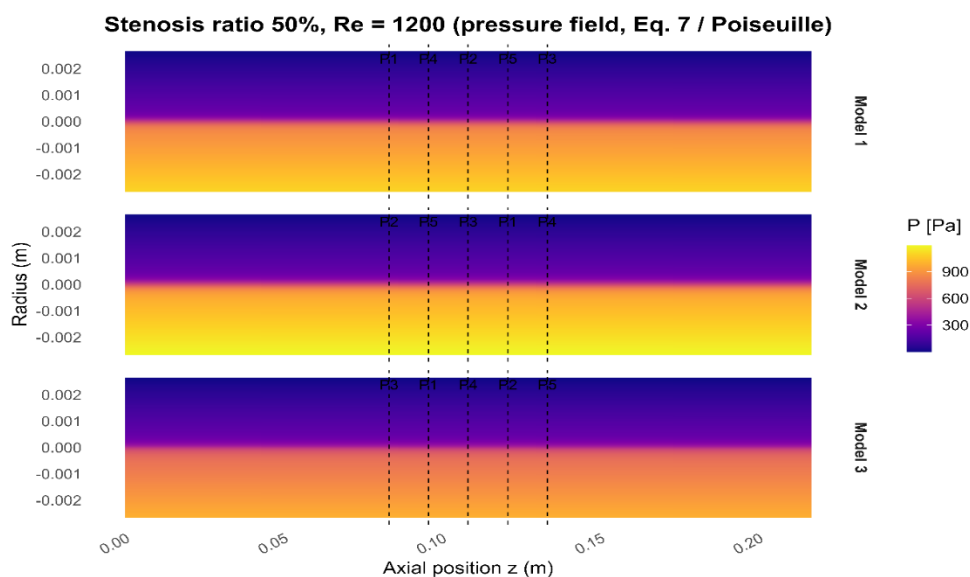


Fig. 6. Pressure field for three stenosis shapes (50% diameter reduction, $Re = 1200$). Axial gradients concentrate within the stenosis; shoulder sharpness controls the distribution of losses. Vertical dashed lines (P1–P5) indicate sampling locations.

Fig. 6 contrasts three stenosis morphologies—cosine (Model 1), Gaussian (Model 2) and wedge (Model 3)—calibrated to the same throat severity (50% diameter reduction) and throat Reynolds number ($Re = 1200$). In all cases the colour field varies predominantly along the axis and is nearly uniform across the section, as expected for laminar, axisymmetric, quasi-1D conditions. Crucially, the *distribution* of the pressure drop depends on shoulder sharpness: the wedge model concentrates loss into a shorter axial interval (steeper local dP/dz), while the Gaussian shoulders smear the gradient over a broader region. This shape sensitivity, already predicted by R^{-4} resistance, explains why equally severe stenoses need not be equally haemodynamically hazardous; geometrically abrupt lesions generate larger local energy dissipation and larger pre-/post-lesion pressure differentials at the same nominal severity. The dashed fiducials (P1–P5) indicate canonical sampling sites for pre-, intra- and post-stenotic interrogation.

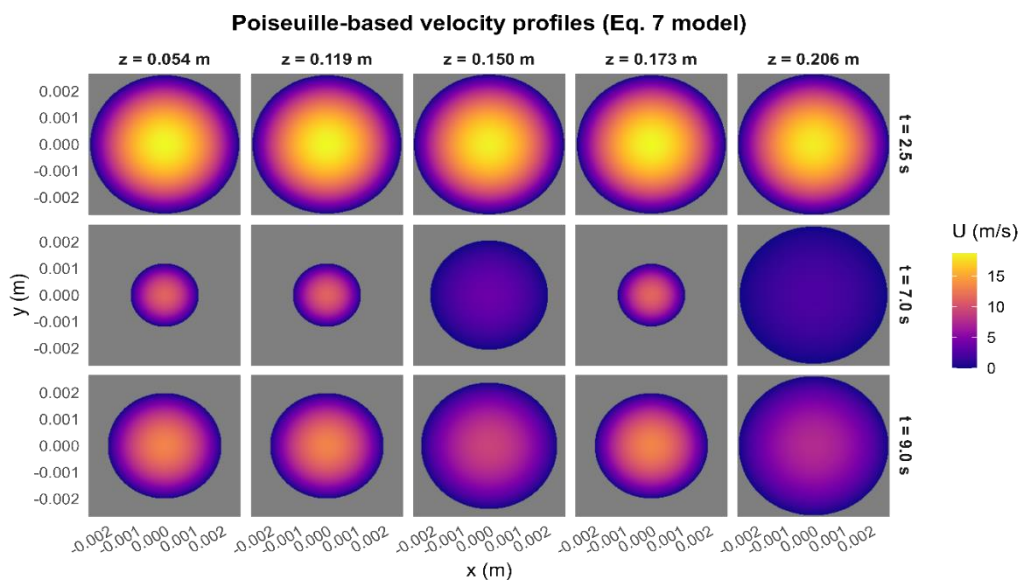


Fig. 7: Cross-sectional velocity profiles at selected times and axial positions. Panels show Poiseuille parabolas compressed during interruptions and restored thereafter.

Cross-sections reconstructed from Eq. (17) (Fig. 7) show the canonical Poiseuille parabola: near-zero velocity at the wall, a single centreline peak and smooth radial decay. During interruptions the field compresses with the lumen, but the peak does not necessarily rise—because $U_{\max}(z, t) = 2Q(t)/(\pi R(z, t)^2)$ reflects the competition of two trends: $R \downarrow$ tends to elevate U_{\max} , whereas $Q \downarrow$ (driven by R^4) tends to depress it. Our simulations lie in the latter regime, giving lower peaks at the most severe constrictions. Away from stenotic regions and outside interruption windows, the larger R and restored Q raise both the width and the apex of the parabola.

The non-dimensional operator in Eq. (17) couples a parabolic velocity kernel to an evolving lumen geometry and a pulsatile pressure driver. Interruption-induced changes in $R_{\text{eff}}(t)$ therefore act *twice*: (i) geometrically, through the quadrature weights over the flow domain, and (ii) hydraulically, via the R^4 resistance law. This dual action yields the coherent signatures observed across modalities, simultaneous minima in $R_{\text{eff}}(t)$, $Q(t)$, $\tau_w(t)$ and $\sigma_\theta(t)$, followed by rapid restitution. From a clinical perspective, such episodes of low τ_w and steep axial pressure gradients highlight risk pathways distinct from average severity alone: short-duration, sharp-shouldered constrictions may exert disproportionate haemodynamic impact.

4.3 Discussion

The findings of this study contribute to the ongoing discourse on blood flow modeling by linking accident-induced carotid artery geometry interruptions to vascular stress, using a modified Poiseuille-based formulation. Simulation results demonstrated that even short-lived constrictions of the carotid lumen caused disproportionately large reductions in volumetric flow rate, consistent with the r^4 scaling law. Furthermore, the model predicted sharp reductions in wall shear stress (WSS) during interruptions despite elevated upstream pressure, highlighting endothelial vulnerability under such

transient conditions. These results provide an analytical framework that extends the utility of classical Poiseuille models to accident scenarios, thereby offering computational efficiency without sacrificing physiological relevance.

When compared with prior empirical works, several linkages emerge. [2] emphasized that simplified Poiseuille models systematically underestimate pulsatile WSS, recommending Womersley-informed corrections to improve accuracy. The present study aligns with these findings by incorporating a Womersley-based pulsatile correction term, which improved representation of flow recovery following interruptions. Similarly, [1] validated numerical approximations of Womersley profiles under idealized conditions, but did not extend their framework to account for sudden trauma-induced deformations. Our findings expand this gap by embedding accident-related geometric penalties directly into the analytical equations, capturing the abrupt variations in flow and shear that conventional pulsatile models overlook.

[7] demonstrated the diagnostic value of patient-specific inverse models for estimating vascular stresses, though at high computational cost. By contrast, the present study offers a lightweight analytical alternative, suitable for rapid assessment in trauma care settings where timeliness is crucial. The proposed model can therefore complement computationally intensive frameworks by offering first-order estimates that are both interpretable and clinically actionable. Similarly, [4] showed that fluid–structure interaction (FSI) approaches effectively capture compliance and wall interactions, but their complexity limits deployment in emergency contexts. Our reduced-order approach addresses this limitation by isolating geometry-driven stress pathways, providing efficient yet physiologically meaningful predictions.

The results resonate with [6], who established that vascular geometry, independent of direct injury, drives long-term remodeling. By demonstrating how transient accident-like constrictions precipitate acute flow penalties and WSS minima, our model highlights the importance of geometry as a first-order determinant of vascular stress under trauma conditions. Unlike Garasic’s chronic stent-focused analysis, the present work situates geometry within acute, dynamic contexts, showing how short-duration constrictions can yield disproportionate hemodynamic consequences.

The findings substantiate and extend the critiques identified in the empirical literature. Existing models either underestimate WSS, assume idealized geometries, or demand computational resources incompatible with clinical exigencies. By bridging these limitations, the present study operationalizes a novel Poiseuille–Womersley hybrid that captures accident-induced geometric interruptions, vascular stress redistribution, and pulsatile flow dynamics. This alignment with both empirical gaps and clinical relevance underscores the model’s contribution to trauma-informed hemodynamic modeling and its potential for integration into stroke prevention and emergency vascular care.

The present framework intentionally neglects wall compliance, secondary flows and non-Newtonian rheology; as a result, transverse pressure gradients, flow separation and oscillatory shear cannot emerge. These simplifications are appropriate for isolating geometry-driven effects in laminar regimes, but they likely understate near-throat complexity at higher Re or in compliant vessels. Extending Eq. (17) with a tube-law (e.g. $P(A)$) and a Windkessel outlet would enable wave–transit effects and phase lags, while non-Newtonian viscosity models could refine shear predictions in low-shear regions. Key haemodynamic signatures captured by the model:

1. Strong flow throttling during interruptions via the R^4 law;
2. Concomitant depressions in τ_w despite elevated upstream pressure;
3. Hoop-stress reductions proportional to the instantaneous radius; and
4. Morphology-dependent axial pressure gradients, with sharper shoulders producing more localised losses.

V. CONCLUSION

This study set out to investigate the impact of vascular stress on carotid artery blood flow during accidents using a novel Poiseuille–Womersley hybrid model. Carotid artery injuries remain a major global health concern due to their association with stroke and trauma-related mortality, and accurate modeling is critical for predicting hemodynamic instability in such conditions. The problem with existing literature is that classical Poiseuille models underestimate wall shear stress, numerical Womersley solutions neglect sudden trauma-induced deformations, and fluid–structure interaction models, while accurate, are computationally intensive and unsuitable for rapid clinical deployment. The findings of this study demonstrate that accident-induced geometric interruptions, such as lumen narrowing or swelling, significantly alter hemodynamics by reducing volumetric flow rate according to the r^4 law, decreasing wall shear stress, and modifying velocity profiles in ways

that cannot be captured by simplified models. The hybrid approach developed here incorporates geometric penalty factors, pulsatile corrections, and localized loss terms to provide physiologically realistic results at reduced computational cost. In conclusion, geometry emerges as a first-order determinant of vascular stress during accidents, and the proposed model offers a tractable yet rigorous analytical framework that bridges clinical usability and theoretical accuracy. For policy, this work highlights the need to integrate vascular stress modeling into trauma diagnostics and emergency response protocols to anticipate cerebrovascular complications. Future research should validate the model with patient-specific imaging, extend it to three-dimensional geometries, and incorporate real-time Doppler measurements to enhance predictive capacity and clinical translation.

REFERENCES

- [1] B. Cortez dos Santos, A. Oizuni, F. Lofrano, P. Blanco, and F. Kurokawa, "Numerical approximation of the womersley problem in openfoam," in *Proceedings of the XLV Ibero-Latin-American Congress on Computational Methods in Engineering (CILAMCE)*, 2024.
- [2] J. Muskat, C. Babbs, C. Goergen, and V. Rayz, "Method for estimating pulsatile wall shear stress from one-dimensional velocity waveforms," *Physiological Reports*, vol. 11, no. 4, p. e15628, 2023.
- [3] S. Chen, H. Zhang, Q. Hou, Y. Zhang, and A. Qiao, "Multiscale modeling of vascular remodeling induced by wall shear stress," *Frontiers in Physiology*, vol. 12, p. 808999, 2022.
- [4] F. Syed, S. Khan, and M. Toma, "Modeling dynamics of the cardiovascular system using fluid-structure interaction methods," *Biology*, vol. 12, no. 7, p. 1026, 2023.
- [5] A. N. Impiombato, G. La Civita, F. Orlandi, F. S. Franceschini Zinani, L. A. Oliveira Rocha, and C. Biserni, "A simple transient poiseuille-based approach to mimic the womersley function and to model pulsatile blood flow," *Dynamics*, vol. 1, no. 1, pp. 9–17, 2021.
- [6] J. Garasic, E. Edelman, J. Squire, P. Seifert, M. Williams, and C. Rogers, "Stent and artery geometry determine intimal thickening independent of arterial injury," *Circulation*, vol. 101, no. 7, pp. 812–818, 2000.
- [7] J. Bracamonte, S. Saunders, J. Wilson, U. Truong, and J. Soares, "Patient-specific inverse modeling of in vivo cardiovascular mechanics with medical image-derived kinematics as input data: Concepts, methods, and applications," *Applied Sciences*, vol. 12, no. 8, p. 3954, 2022.
- [8] S. Kpuduwei, E. Kiridi, H. Fawehinmi, and G. Oladipo, "Reference luminal diameters of the carotid arteries among healthy nigerian adults," *Folia Morphologica*, vol. 81, no. 3, pp. 579–583, 2022.
- [9] E. Soleimani, M. Mokhtari-Dizaji, N. Fatouraee, and H. Saberi, "Assessing the blood pressure waveform of the carotid artery using an ultrasound image processing method," *Ultrasonography*, vol. 36, no. 2, p. 144, 2017.
- [10] K. Soueidan, S. Chen, H. R. Dajani, M. Bolic, and V. Groza, "The effect of blood pressure variability on the estimation of the systolic and diastolic pressures," in *2010 IEEE International Workshop on Medical Measurements and Applications*, pp. 14–18, IEEE, 2010.
- [11] R. S. Seymour, Q. Hu, and E. P. Snelling, "Blood flow rate and wall shear stress in seven major cephalic arteries of humans," *Journal of Anatomy*, vol. 236, no. 3, pp. 522–530, 2020.
- [12] F. A. Choudhry, J. T. Grantham, A. T. Rai, and J. P. Hogg, "Vascular geometry of the extracranial carotid arteries: an analysis of length, diameter, and tortuosity," *Journal of neurointerventional surgery*, vol. 8, no. 5, pp. 536–540, 2016.
- [13] D. J. Vitello, R. M. Ripper, M. R. Fettiplace, G. L. Weinberg, and J. M. Vitello, "Blood density is nearly equal to water density: a validation study of the gravimetric method of measuring intraoperative blood loss," *Journal of veterinary medicine*, vol. 2015, 2015.
- [14] W. Lee, "General principles of carotid doppler ultrasonography," *Ultrasonography*, vol. 33, no. 1, p. 11, 2014.
- [15] E. Nader, S. Skinner, M. Romana, R. Fort, N. Lemonne, N. Guillot, A. Gauthier, S. Antoine-Jonville, C. Renoux, M.-D. Hardy-Dessources, *et al.*, "Blood rheology: key parameters, impact on blood flow, role in sickle cell disease and effects of exercise," *Frontiers in physiology*, vol. 10, p. 1329, 2019.